Energies **2015**, *8*, 6738-6764; doi:10.3390/en8076738

OPEN ACCESS

energies

ISSN 1996-1073

www.mdpi.com/journal/energies

Article

Models of Talik, Permafrost and Gas Hydrate Histories—Beaufort Mackenzie Basin, Canada

Jacek Majorowicz [1,*], Kirk Osadetz [2,†] and Jan Safanda [3,†]

[1] Northern Geothermal Consult, 105 Carlson Close, Edmonton, AB T6R 2J8, Canada

[2] Containment and Monitoring Institute (CaMI), CMC Research Institutes Inc., 3535 Research Road NW, Calgary, AB T2L 2K8, Canada; E-Mail: kirk.osadetz@cmcghg.com

[3] Institute of Geophysics, Czech Academy of Science, Prague 14131, Czech Republic; E-Mail: jsa@ig.cas.cz

† These authors contributed equally to this work.

* Author to whom correspondence should be addressed; E-Mail: majorowicz@shaw.ca; Tel./Fax: +1-780-438-9385.

Academic Editor: Enrico Sciubba

Received: 17 March 2015 / Accepted: 23 June 2015 / Published: 30 June 2015

Abstract: Models of talik, permafrost and gas hydrate (GH) histories below shallow lakes are investigated and compared to models of Beaufort Mackenzie Basin (BMB) GH occurrences to describe lacustrine inundation effects, which are compared against factors controlling the variations among Mackenzie Delta (MD) permafrost, GH and talik occurrence. Models using a 2–4 °C boundary temperature range indicate that geological setting, specifically underlying lithology and porosity, are the primary controls in talik formation below lakes. Below a lake of any size, where the underlying lithology is sandy it is practically impossible to produce a pervasive talik or to completely degrade significant GH accumulations in response to the boundary condition thermal effects alone. Models predict that talik formation is, in such cases, restricted to the upper few tens of meters below the lake. Permafrost degradation appears common where porosities are <40% and water bottom temperatures reach 2–4 °C, in both marine and lacustrine settings. Where porosities are higher a thin GH stability zone can persist, even where deep taliks have formed.

Keywords: gas hydrates; permafrost; Beaufort-Mackenzie Basin; taliks

1. Introduction

Lakes cover between 20% and 50% of the Mackenzie Delta landscape (Figure 1), to the extent that landscape evolution is inferred to have played an important role in conditioning ground temperatures. Warmer ground temperatures beneath lakes affects the proportion of liquid water *versus* ice within the matrix pore space [1–3]. Lakes, which are generally inferred to have formed after 6 ka ago, produce warmer ground temperatures. Following lacustrine inundation the inferred ground temperature changes from approximately −15 °C, at the end of the last Ice Age, to the lake bottom temperature of 2.3 °C [1] or higher (2 °C–4 °C; Burgess *et al.* [4]; Burn [5]) which effects the underlying permafrost and methane gas hydrates (GH).

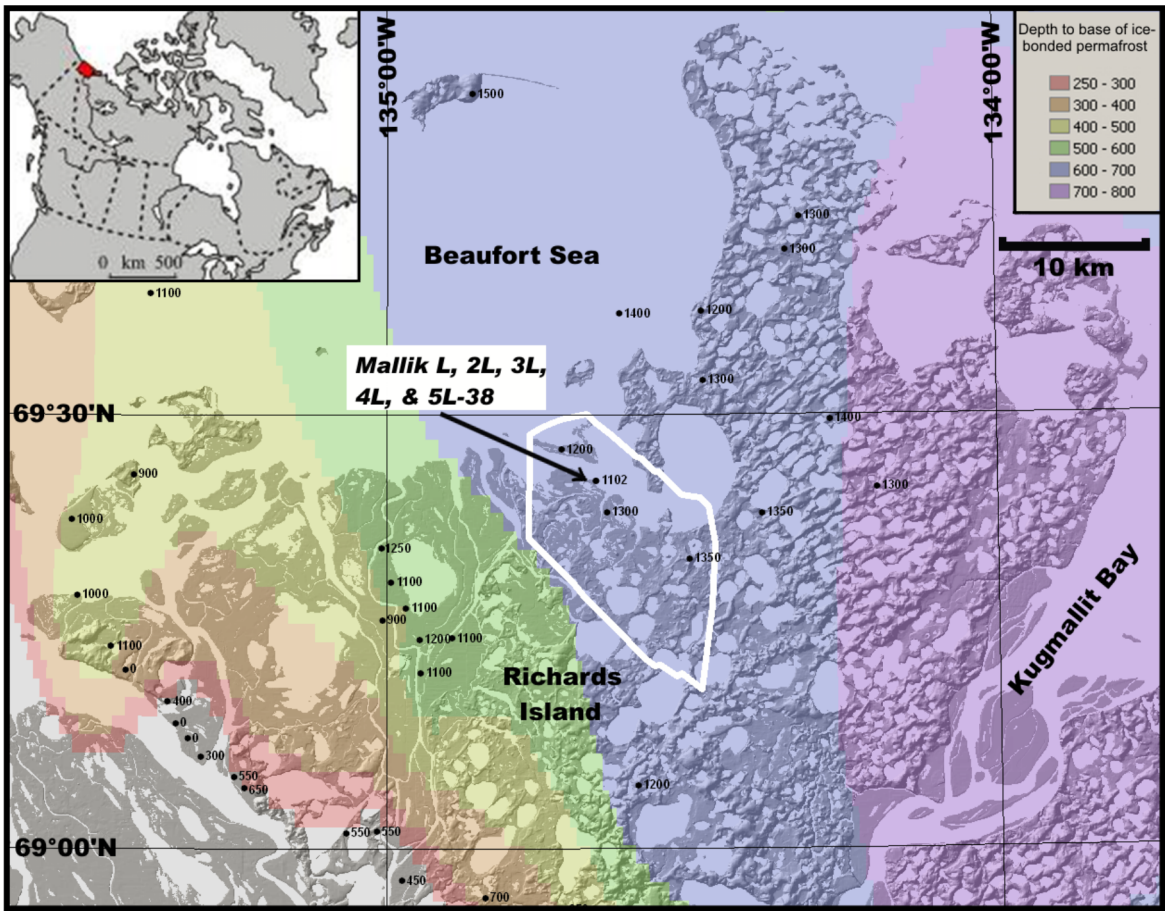

Figure 1. Study area and Mallik GH field location (according to [2]). Numbers posted by black dots (wells) are depths (m) to base GH stability [6].

When the Beaufort Mackenzie Basin (BMB) permafrost and GH occurrences offshore are compared to those onshore, particularly below lakes, the occurrences appear paradoxical. Thick permafrost and GH layers or indicators for their presence occur in wells and seismic data both onshore and offshore. Offshore relict terrestrial permafrost and GH that formed during the Pleistocene sea level low-stand are degrading slowly following Holocene marine transgression. Onshore MD locations like Mallik have thick permafrost and GHs that also are degrading slowly in response to Holocene ground surface warming. In contrast taliks typically lacking indications for GH occurrences are inferred to occur commonly below shallow lakes. Onshore seismic tomography inversion from direct arrivals indicates

low velocities extending down to 300 m, in some places, commonly under lakes [2] and these are inferred to be taliks that formed under lakes during recent interglacial history [1].

Why should taliks form below young, shallow lakes while submarine permafrost and GHs persist and degrade slowly below areas inundated by Holocene marine transgression? To explore this interesting and paradoxical situation we model "thermokarst" effects below lakes and compare it to the effects of Holocene marine transgression.

Study area lakes are geologically ephemeral (*i.e.*, <6 ka old) and generally very shallow. Lakes can affect both the landscape and subsurface environments including the formation of pingoes where these ephemeral lakes have been drained. Therefore it is reasonable to assume that these Holocene lakes can potentially affect permafrost and GH formation and preservation. In the marine setting, by comparison, up to ~100 m of water has flooded, since ~8 ka ago, the continental shelf exposed previously during the low stand at the last glacial maximum Yet relict permafrost and GHs that are sometimes very thick persist below the shallow Beaufort Sea [6–8]. We compare three model settings of BMB region permafrost and GH stability including:

1. A terrestrial onshore model, essentially like the Mallik site that we modelled previously [9,10];
2. A marine offshore model similar essentially to the Adgo P-25 well, where thick relict permafrost and GH developed during the Pleistocene low stand persist since >8 ka ago; and
3. An onshore model beneath lakes < 6 ka old similar to those interpreted to be underlain by talik (Figure 2).

In the onshore case, many factors can influence talik formation below lakes beyond the effects of a simple change in ground surface or lake bottom temperature compared to a standard terrestrial setting like the Mallik location. These factors include water body temperature, time since inundation that we know is variable because of the presence of pingoes, as well as, the previous surface temperature history, pore water composition, lithology, porosity, thermal conductivity, heat flow among other factors. The two onshore models provide a clear opportunity to compare the lacustrine and terrestrial onshore environments, while the comparison with areas inundated by Holocene sea level rise indicates the different effects of terrestrial and marine inundation.

Previous analyses of MD talik formation below Holocene lakes developed on a permafrost landscape were based on modeling of the related sub-lake geothermal regime [1]. Taylor *et al.* [1] presented a two-dimensional finite element geothermal model that simulated talik formation beneath lakes of various diameters and variable underlying lithology, using a surface history that assumed a thermal steady-state at the end of the Wisconsin, subsequently affected by transient effects accompanying Holocene warming and mid-Holocene lake formation. Their models assumed that lakes first formed 6 ka ago [1]. These models did not consider the presence or potential influence of underlying GHs on the permafrost model history. We build on this well researched surface forcing model to elaborate talik development adding the effects on permafrost and talik dynamics of GH presence and stability.

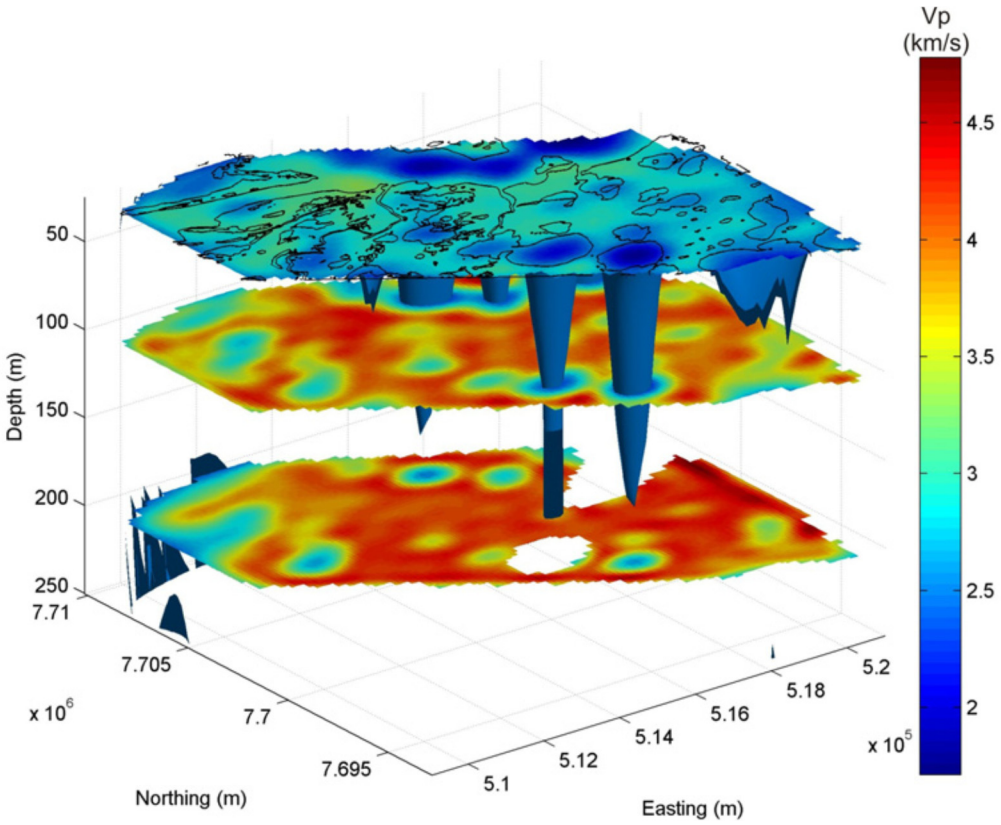

Figure 2. Tomographic inversion of direct seismic arrivals indicating inverted-cone shaped regions of lower velocities underneath lakes and other surface drainage, some extending to depths of ~300 m [2].

Lake bottom temperatures can vary between 2 and 4 °C [1,5]. Taylor *et al.* [1] assumed 2.3 °C based on previous research, as described next. Burgess *et al.* [4] artificially drained Illisarvik Lake on Richards Island in order to investigate permafrost growth. Twenty-four boreholes instrumented with temperature cables were drilled to depths between 15 and 92 m below lake level in order to monitor ground temperature profiles beneath the lake its environs. Work that preceded the drainage of the lake delineated the presence of a bow-shaped talik extending up to 32 m below the lake bottom. They characterized the pre-drainage temperature and post-drainage temperature profiles in the central lake holes as follows:

(i) An upper unfrozen horizon in which temperatures reached a maximum of 2.3 °C at roughly 5 m below lake bottom;
(ii) A permafrost layer at depths of 20 to 32 m in the central part of the lake with consistently negative temperatures below;
(iii) Negative temperature gradients below the 5 m maximum temperature, averaging 50 mK/m in the permafrost section;
(iv) The pre-existing talik was completely frozen near the lakeshore sites (*i.e.*, <10 m water) two years after draining the lake.

Burn [5] showed that these lakes, on average 33 ha size, occupy a quarter of the surface area of Richards Island, Northwest Territories (Figure 1). Most of the lakes have a central pool deeper than the thickness of winter ice, and many have prominent, shallow, littoral terraces. The relatively warm lake bottom temperatures cause considerable disturbance of the surrounding continuous permafrost. Water

and lake-bottom temperatures, the configuration of permafrost, and active-layer thickness were measured at a tundra lake between 1992 and 1997. The lake they studied is oval, 1.6 km long, 800 m wide, and as deep as 13 m. Sandy terraces, covered by less than 1 m of water, extend more than 100 m from the contemporary shoreline. The terraces are underlain by permafrost that terminates almost vertically at their lake-ward limit. The annual mean temperature measured at the lake's bottom in the central pool ranged between 1.5 °C and 4.8 °C, depending on depth, and between −0.2 °C and −5 °C on the terraces, due to differences in snow cover and their proximity to the central pool. In consequence, the temperature of permafrost at 7 m depth in the terraces also varied, from −2 °C near shore to −5 °C in the middle of the terrace field. The active layer in the terraces was uniformly 1.4 m deep.

Geothermal modeling of talik configuration indicates no permafrost beneath the central pool of the lake. Based on model results they inferred that, under equilibrium conditions, about one quarter of the lakes on Richards Island are underlain by taliks that penetrate the permafrost, and that such talik conditions might underlie at least 10%–15% of the area of Richards Island. Short-term climate changes predicted for the region imply a small increase in summer lake water temperature and an extension of the open-water season, accompanied by thicker winter snow cover. Following such changes, with a longer freeze-up interval and warmer winter terrace temperatures they suggested that, the future, permafrost might not persist under the fringing lake terraces.

Previous work suggested that thermal taliks (>0 °C) develop quickly beneath lakes [1], They found a strong temperature dependence on the unfrozen water content where the sediments underlying the lake were finer-grained, and the volume of pore filling ice-bonding is reduced. Such that, where the underlying lithology is fine-grained clayey silt, the sediments beneath the talik developed elevated unfrozen water contents that eventually extended to the base of permafrost, forming chimney-like structures of partially ice-bonded soils penetrating beneath the larger lakes. In contrast, where the underlying lithology is highly porous sand, where, the sediments beneath the talik remain almost entirely ice-bonded to the present as a result of the pore space ice content.

2. Models

2.1. Onshore Reference Model—Mallik Area

We compare the two inundated setting models against the well described terrestrial onshore Mallik model where we previously employed a temperature history [10] that assumed that the equivalent current Vostok ΔT temperature of 0 °C corresponds to a present ground surface temperature of −6 °C at the Mallik site. This permitted us to infer a Mallik GST (ground surface temperature) oscillation history between −6 °C and −4 °C for the period 6–3.5 Mya. The oscillation period seems to be close to 41 ka ago, the same as that observed later between 2.5 through 1 Mya.

We found that the variations of GSTs between −6 °C and −4 °C is critical for model GH formation histories (Figure 3). The steady-state profile corresponding to the best Mallik geothermal model (basal heat flow density 60 mW/m^2, conductivity of frozen × unfrozen rock 3.4 × 2.1 W/(m·K) approaches the GH phase curve from above at the depth of about 300 m when the GST is −5 °C. Figure 3 indicates that GH could not have formed if GST was higher than −5 °C. The equilibrium permafrost thickness is ~250 m if GST is −5 °C, indicating that the permafrost, which forms a commonly

impermeable lid to gas migration, existed long before the downwardly propagating cooling that resulted in *p–T* conditions that enabled formation of the first GHs.

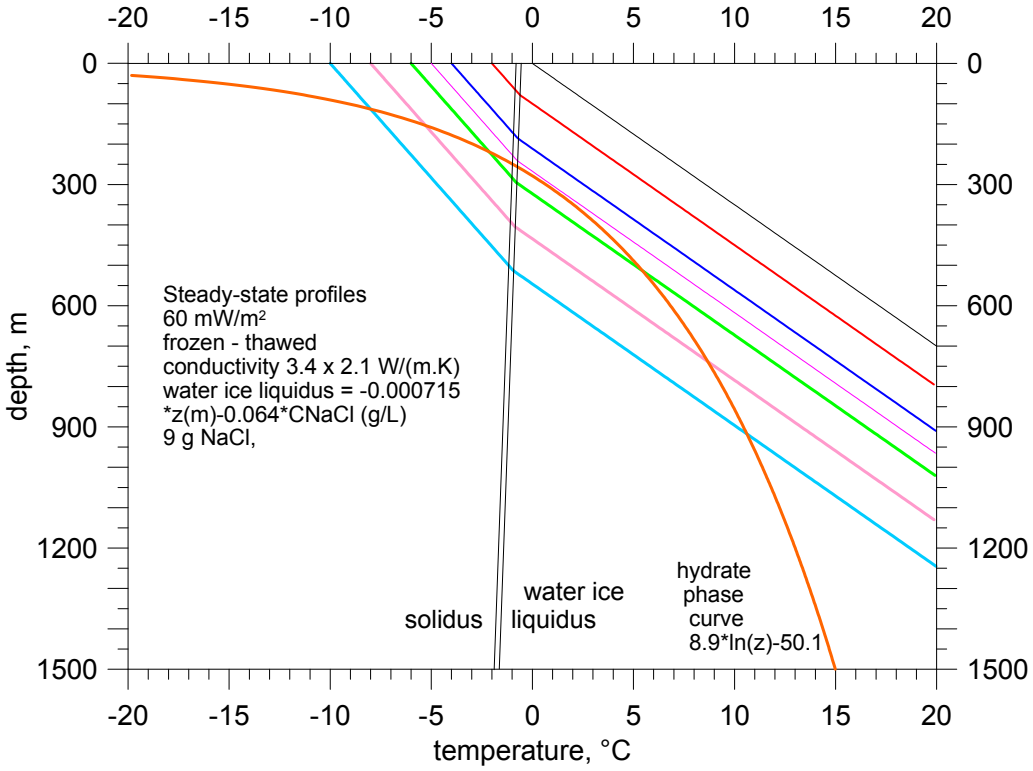

Figure 3. Steady-state profile corresponding to the best Mallik geothermal model (basal heat flow density 60 mW/m^2, conductivity of frozen × unfrozen rock 3.4 × 2.1 W/(m·K)) and various possible ground surface temperatures of: 0, −2, −4, −5, −6, −8 and −10 °C.

Accordingly, GST history indicates that the first GH began forming at 5.96 Mya and that it reached its maximum thickness of 130 m, at depths between 250 and 380 m, shortly after the GST change from −5.5 °C to −4.5 °C, about 5.5 Mya. The permafrost penetrates into the GH layer only 9 m, between 250 and 259 m deep. Following the GST warming, the last GH dissipated from a depth range of 310–340 m at time 5.47 Mya (Figure 4) when it was separated from the base of the permafrost, which was at a depth of 240 m, by a 70 m thick melted zone. GH formed subsequently after the next decrease of GST from −5.0 °C to −5.5 °C at about 4.5 Mya. Subsequently the GHs persisted through all other GST variations to the Present. The upper constraint imposed by the overlying permafrost at 250 m was always within the GH stability zone and its maximum extent was to a depth of 990 m, which was reached during the most recent glacial epoch. These simulations of GH stability zone histories considered the thermal conductivity and heat capacity of GH as well as the latent heat of the GH formation and dissipation.

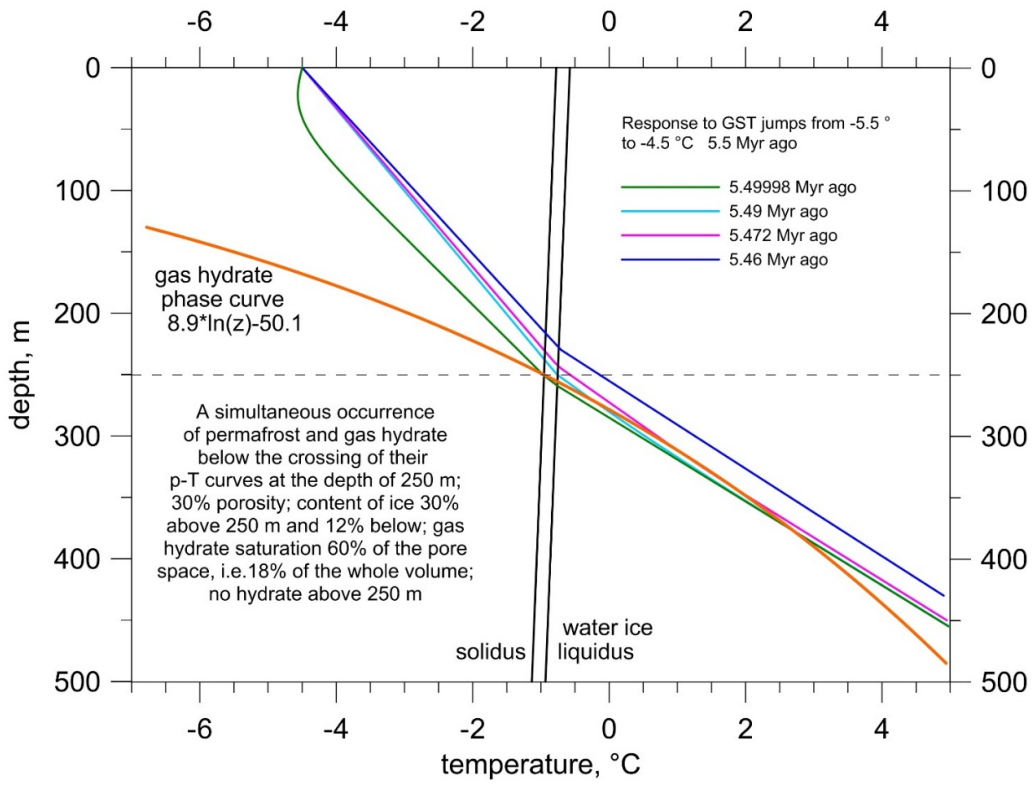

Figure 4. Transient temperature–depth profiles as a response to the sudden GST warming from −5.5 °C to −4.5 °C, 5.5 Mya (and to all previous GST changes since 14 Mya). The profiles correspond to times 20, 10 ka, 28 ka and 40 ka after the warming began. Curves for 28 ka illustrate the moment when the last GH dissipates in the depth interval 310–340 m, separated from the permafrost base at the depth of 240 m by a 70 m thick melted zone.

2.2. Offshore Beaufort—Sea Holocene Marine Transgression Model

The marine transgression model, that includes a projected future warming due to global change extending 300 years into the future, is consistent with the observed presence of GHs that are stable below a relict permafrost in the Beaufort Sea (Figure 5 below). In that model the permafrost is melting both from above and from below with an attendant latent heat effect. Because of this buffering, the latent heat effects that accompanying the melting permafrost has the effect of increasing the stability of the GHs, which remain stable into the future even where an inferred future doubling of atmospheric CO_2 induces a GST warming between 1 °C and 7 °C.

The lithological structure of this model is predominantly sandy, with 30% porosity, which is either ice or water filled, such that the sediment thermal conductivities are 3.4 and 2.1 W/(m·K), respectively. The resulting water column exerts a higher pressure that expands the depth range of the GH stability both to shallower and deeper depths below the top of the sedimentary succession (compare the 50 m and 70 m water depth models shown in Figure 5).

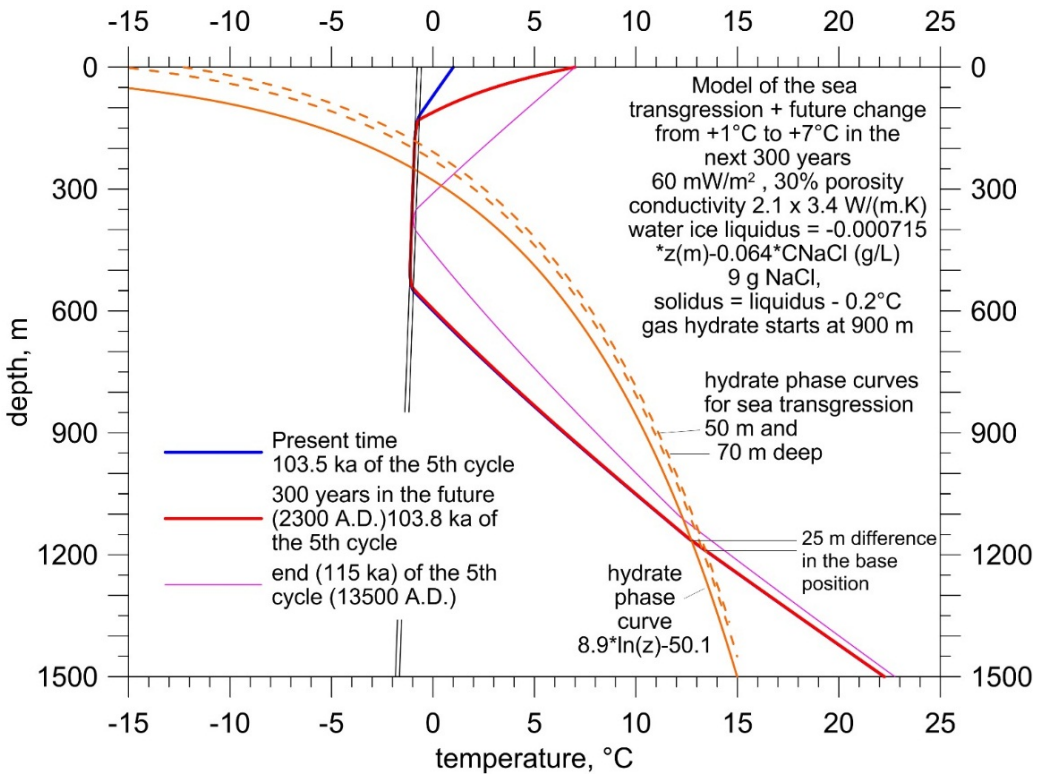

Figure 5. Offshore Beaufort model results where the marine transgression water depths are either 50 m or 70 m. Note that relict permafrost and GH remain stable in this BMB model.

2.3. 2-D Mackenzie Delta Models of Onshore Lakes

These simulations are based on a numerical solution of the heat conduction equation by finite differences [11] in 2-D or axis-symmetric geothermal models, accounting for the latent heat of the water to ice phase changes. The 2D code used for the talik simulations is that of Safanda, which was first used in [12]. Analytically exact and approximate solutions of various freezing and thawing problems have been addressed using this code previously [13,14]. These solutions are applicable to certain basic situations such as freezing of a half-space with initial temperature gradient, or freezing and thawing of a layer at initial freezing temperature. The numerical simulations were done by solving the transient heat conduction equation in one- and two-dimensional situations in a porous medium. The implicit scheme of the finite-difference method ([15]) was supplemented with an algorithm enabling the latent heat of the subsurface water–ice transition to be modelled in a manner similar to the latent heat of magma crystallization [16].

The depth grid steps increase from the surface downward from 2 m to 5 m, 10 m, 25 m, 50 m, 100 m and 250 m in depth layers 0–100 m, 100–200 m, 200–500 m, 500–1000 m, 1000–2700 m, 2700–5000 m and 5000–10,000 m. The horizontal grid steps vary between 5 m and 100 m with highest density around the lake rim and the largest step close to the rim of the model, usually 4–6 km away from the lake's rim. The upper boundary condition is the temporally varying ground surface temperature, and the lower boundary is a constant heat flow density of 60 mW/m^2 at 10 km [17–20].

The simulations included consideration of the latent heat of interstitial water or ice either freezing or melting on the limit of the permafrost stability zone. Taylor *et al.* [1] consider a dynamic ice model, but they did not include any consideration of GHs in their models. In our models we also consider the impact

of GH presence and stability. However, unlike the reliably ubiquitous occurrence of ice bonded permafrost the occurrence of which is practically certain for pore space water under the proper *p–T* conditions, the presence of methane in the pore space is not guaranteed and so the presence of GH stability cannot be inferred indicative of GH occurrence. This is why the geothermal models used in the models below do not consider GH properties in the GH stability zone.

During the simulations, we determined the permafrost surface and the permafrost base in each time step. In the clayey lithological model, the interstitial ice dissipates gradually between the depth dependent temperatures of *solidus* and *liquidus*, *i.e.*, over a broad interval of 2 °C. In all simulations, the permafrost surface and permafrost base were determined as the depths, where the temperature equalled the mean value between the *solidus* and *liquidus* for the given depth at a given time. In each time step, we also determined the depth range of possible GH stability.

2.3.1. Rock Parameters

Following [1] we considered two different lithology types that are typical of MD lake bottom sediments—sand or clayey silt. Similar to our previous permafrost simulations in the BMB and MD, the properties of sand were: 30% porosity with all pore water frozen when below solidus temperature, thermal conductivity 3.4 W/(m·K) in permafrost and 2.1 W/(m·K) outside it, specific heat 2.38 MJ/m^3 in permafrost and 3.06 MJ/m^3 outside.

Properties of the clayey silt lithology [1] are: 48% porosity and 80% water frozen when below solidus, thermal conductivity 2.0 W/(m·K) in the permafrost and 1.2 W/(m·K) outside it. The specific heat is 2.48 MJ/m^3 in permafrost and 3.35 MJ/m^3 outside it. Thermal conductivity and specific heat vary linearly from "permafrost" values to "thawed" values between the *solidus* (T_{sol}) and *liquidus* (T_{liq}) temperatures. Values of T_{sol} and T_{liq} were −0.2 °C and +0.2 °C, respectively, in sand and −2.5 °C and −0.5 °C, respectively, in clayey silt. T_{sol} and T_{liq} are depth and salinity dependent. They decrease with increasing depth at a rate 0.000715 K/m, and decrease with increasing salinity at a rate 0.064 K per gram of the dissolved salt per litre of pore water.

We used a wider range of clayey silt porosities than that considered previously [1] was considered herein. We assume that porosities between 30% and 48% in various models to test the effect of porosity upon talik formation, permafrost history and GH stability. We use a constant salt concentration of 9 g/L.

2.3.2. Surface Forcing Model

The model lake and underlying talik simulations start at an initial steady-state temperature–depth profile corresponding to a ground surface temperature of −15 °C prior to 13.5 ka ago. At that time the temperature jumps to −2 °C. Later it jumps to −5 °C at 8 ka ago and then to −6 °C at 4.5 ka ago. The formation and existence of a lake was simulated by an increase of the surface temperature from −2 °C to +2.3 °C model [1] at the future site of the model lake beginning 10 ka ago. We also considered a warmer model lake by changing to +3 °C or to +4 °C.

Taylor *et al.* [1] assumed a steady-state initial *T–z* profile corresponding to surface temperature of −15 °C. We used this model for a series of the initial computations, but we explored also the implications of a transient initial temperature profile beginning at 13.5 ka ago, that provides a model that coincides with the end of the last ice age.

The simulations start at with an initial steady-state temperature–depth profile corresponding to a ground surface temperature of −15 °C prior to 13.5 ka ago immediately prior to the earliest possible formation of a lake. At that time the temperature jumps to −2 °C. Later it jumps to −5 °C at 8 ka ago and then to −6 °C at 4.5 ka ago. The formation and existence of a lake was simulated by a jump of the surface temperature from −2 °C to +2.3 °C model [1] at the site of the lake 10 ka ago. We also considered a warmer lake by changing to +3 °C or to +4 °C (see Figure 6 below).

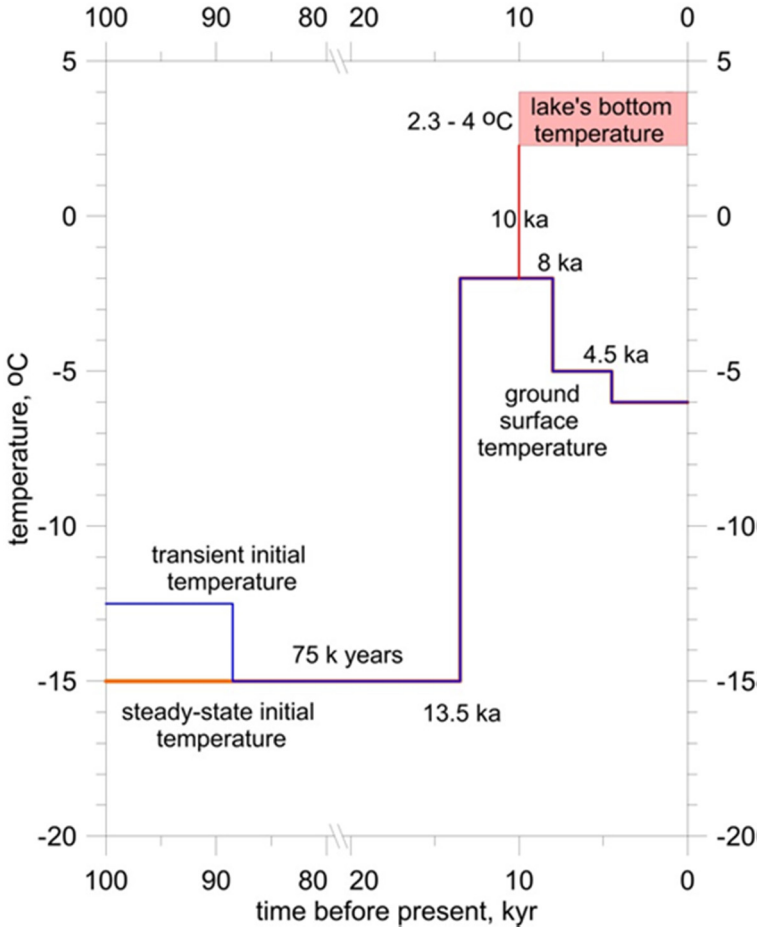

Figure 6. "Temperature history". The time–varying ground surface temperature used as a boundary condition in the simulations that start by jump from −15 °C to −2 °C at time 13.5 ka, followed outside a lake by cooling to −5 °C and −6 °C at times 8 ka and 4.5 ka, respectively. At the time of a lake origin, 10 ka, the ground temperature at the site of a lake warms up from −2 °C to +2.3 °C (or to +3 °C or +4 °). The steady-state initial *T*–*z* profile at time 13.5 ka corresponds to the surface temperature of −15 °C, the transient initial *T*–*z* profile to the temperature history shown by the "transient initial temperature" curve (see text in Section 2.3.4).

Lake history data from other areas, like Canadian Yukon indicate that 11.5 ka provide a models time close to upper limit of when models could commence. Western Canadian Arctic thermokarst lakes also developed in the early Holocene. A 727 cm long lake sediment core was analysed for radiometric ages, magnetic susceptibility, granulometry, and biogeochemical characteristics (organic carbon, nitrogen, and stable carbon isotopes). Based on eight calibrated Accelerator Mass Spectrometry (AMS)

radiocarbon dates, the sediment record covers the last ~11,500 years. The lake bottom sedimentary record was divided into four litho-stratigraphic units reflecting different thermokarst stages. Thermokarst initiation began ~11.5 cal ka BP (Before Present). Between ~11.5 and 10.0 ka BP, lake sediments of unit A accumulated in an initial lake basin created by the combined effects of the melt of massive ground ice and subsidence due to thawing. Between 10.0 and 7.0 ka BP (unit B) the lake basin expanded in area and depth, an effect that was attributed to talik formation during the Holocene thermal maximum, when higher-than-modern summer air temperatures led to increased lake productivity and widespread terrain disturbances in the lake's catchment [21].

2.3.3. The Influence of Lithology, the Influence of Lake Size and Symmetric *vs.* Axis-Symmetric Models

We modelled both sandy and clayey silt lithological substrate conditions. For the sandy lithological models the dissipation of permafrost and possible GH is practically impossible below a lake of any size due to the thermal effect of the lake. There is, however the possibility of forming a shallow, up to 0.2 km talik, under the centre of the lake (see Figure 7 upper panel).

The results for the clayey lithological models are strongly dependent on the mechanical compaction and sediment porosity. The modelled permafrost and GH do not dissipate completely below lakes where the clayey substrate has a high porosity of 48% (*cf.* [1]), which represents a model with little compacted sediment. Both the permafrost and GH dissipate completely in models where the porosity is lower, 30%, which represents a more compacted sediment model (Figure 7 upper *vs.* lower panels, respectively).

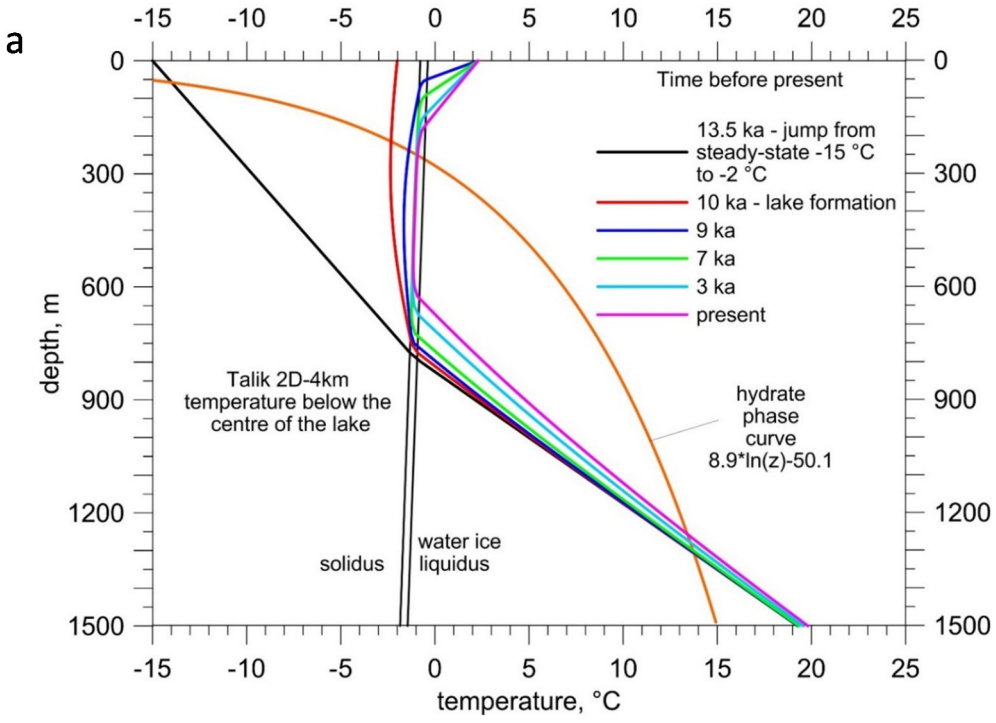

Figure 7. *Cont.*

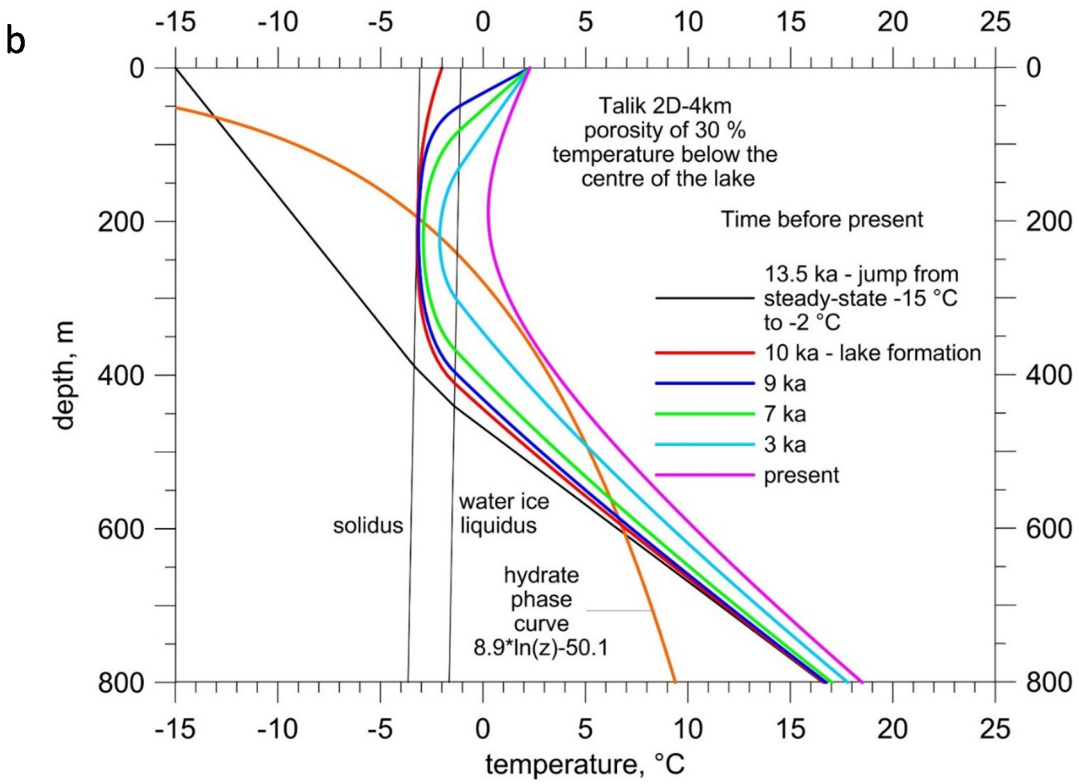

Figure 7. Temperature–depth modeled profiles for 13.5 ka ago, 10 ka ago, 9 ka ago, 7 ka ago, 3 ka ago and Present *vs.* stability phase boundaries for permafrost and methane GH, (**a**) Sands (30% porosity); (**b**) clayey silt (30% porosity).

We have also considered influence of the lake size and symmetric *vs.* axis-symmetric models which are shown in the Appendix. These models show that the effect of increased lake width, up to at least 10 km, has no significant effect on the depths of the permafrost and GH stability layers in the models. From this we conclude that once lakes are 4 km wide, or larger, they are sufficiently large for the temperature below their center to become independent of the temperature distribution in the land beyond the lake margin. As expected, consideration of a circular lake instead of a 2-D infinite lake diminished the warming effect affecting talik formation significantly. The predicted talik zone is thinner by some 50 m for the 30% porosity sand when a circular lake model is considered. The effect on the permafrost base between the two models is much smaller, <20 m. The effect on the model GH base is insensitive to lake geometry (see Appendix).

2.3.4. Influence of the Initial Transient Temperature–Depth Profile

We explored, as mentioned in Section 2.3.2, the effect on simulations of a transient initial temperature–depth profile beginning 13.5 ka ago instead of using the steady-state initial profile with surface temperature of −15 °C. Our previous calculations [9,10] showed that the temperature at the end of the last ice age was not in equilibrium with the −15 °C surface temperature. In the glacial cycle the length of the cold phase is not sufficiently long for the permafrost to reach its full thickness. In this sense, simulations of the permafrost and GH decay below lakes for models with an initial temperature profile at 13.5 ka which assumed a steady-state surface temperature of −15 °C [1] tend to overestimate both the thickness of permafrost and gas hydrate layers and the time necessary for their dissipation.

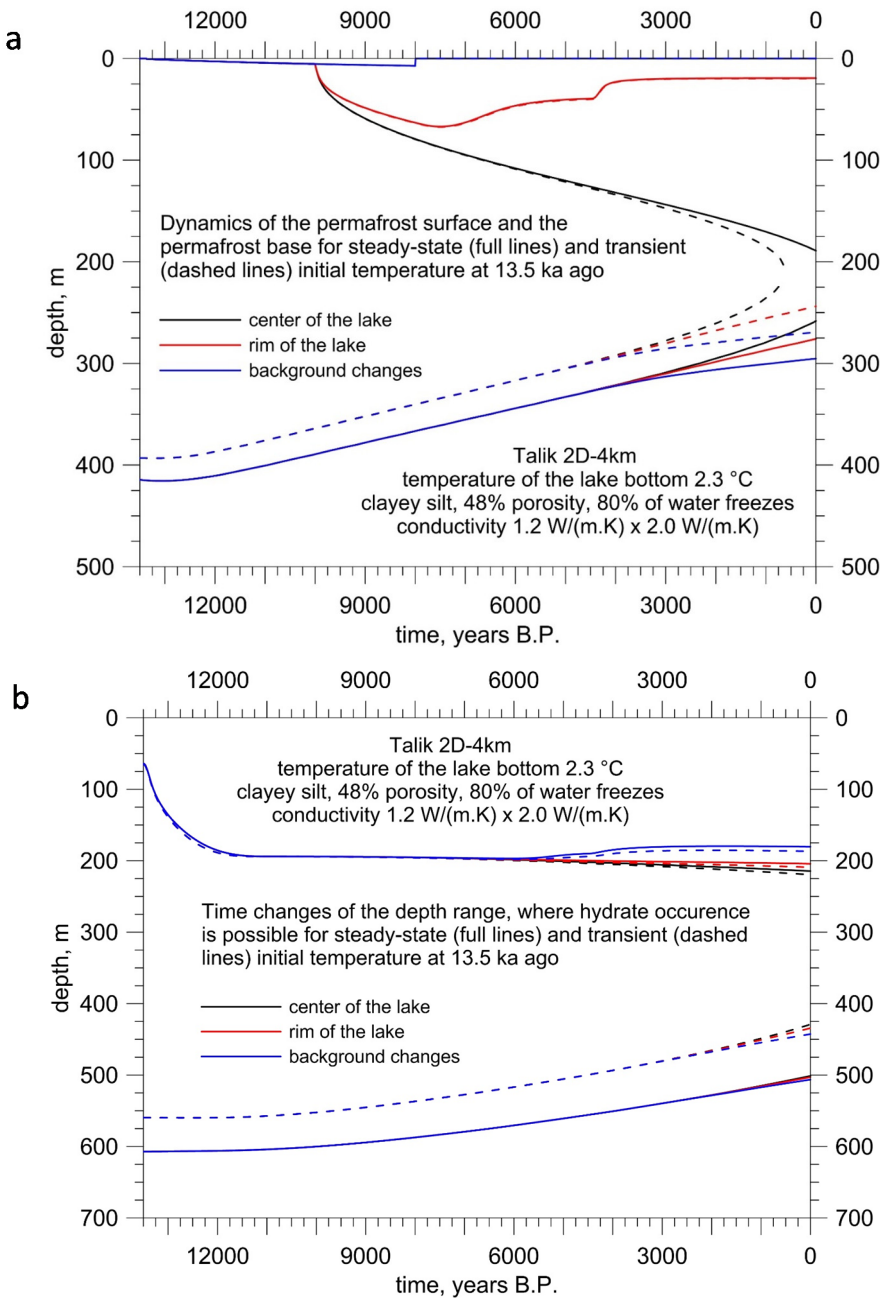

Figure 8. Model results for the steady-state and transient initial surface temperature forcing beginning at 13.5 ka ago for both the permafrost boundaries (**a**) and the GH boundaries (**b**).

The transient *T*–*z* profile used was obtained by solving the 1-D problem for the first 75 ka of the 100 ka glacial cycle, the mean temperature of which is −12.5 (an average of −15 °C for the 75 ka long cold part and temperatures between −6 °C and −2 °C for the remaining 25 ka of interglacial, following Taylor *et al.* [1]. As a result, the simulation started by moving quickly from −12.5 °C to −15 °C and followed by slower temperature changes during the subsequent 75 ka. In Figure 8 we show the temporal dynamics of permafrost and that of the GH in the 48% porosity clayey model both for the steady-state and transient initial *T*–*z* profiles. The model with an initially transient *T*–*z* profile predicts shallower permafrost and gas hydrate layer bases, several tens of meters shallower than those obtained using a steady state temperature profile. They also predict times that are 1–2 ka earlier for the decay of permafrost below the lake than doe the steady state temperature profiles.

It should be stressed here that in the clayey lithology, the interstitial ice dissipates gradually between the depth dependent temperatures of *solidus* and *liquidus*, *i.e.*, in a broad interval of 2 °C [1]. In all simulations, the top and bottom limits of the permafrost are determined as the depths at which the temperature equals the mean value between the *solidus* and *liquidus* at any given time. That is why the *T–z* curves shown in the figures below can be within the *solidus–liquidus* interval, whereas the temporal and spatial dynamics of the permafrost boundaries depicted in the figures indicate current permafrost dissipation. In such models the minimum value of the corresponding *T–z* profile is higher that the *solidus–liquidus* mean temperature. For the clayey model, the *T–z* profiles below the center of, a 4 km wide lake with a 2.3 °C lake bottom temperature (similar to conditions in Taylor *et al.* [1]) are shown in Figure 9.

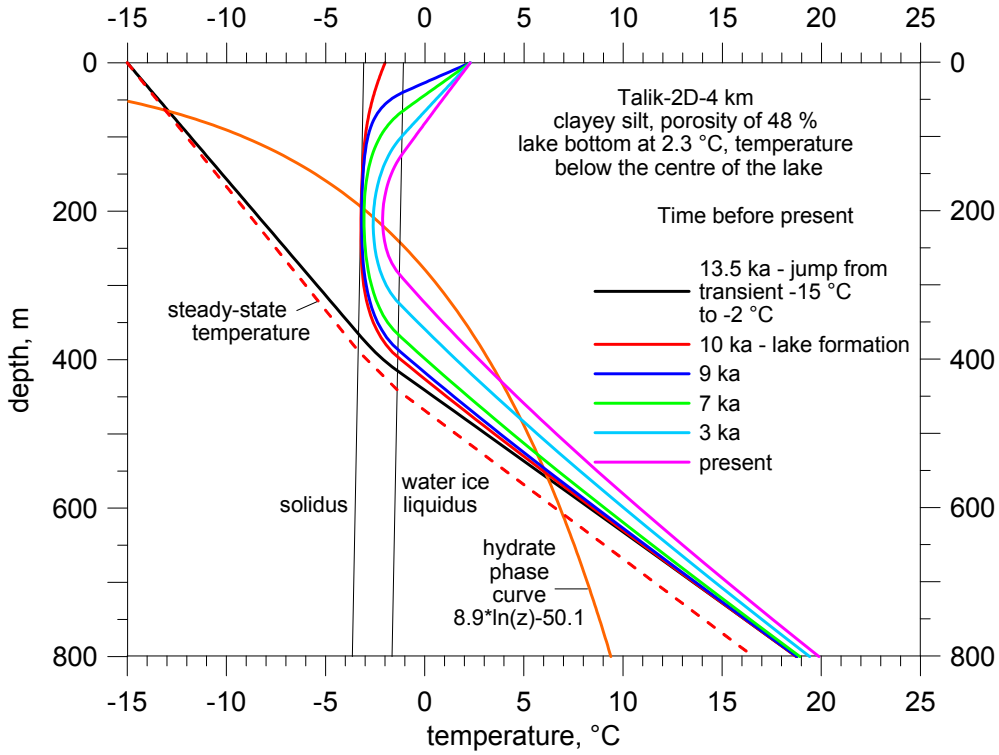

Figure 9. *T–z* profiles for the center of the lake at its formation 10 ka ago, and at 9 ka ago, 7 ka ago, 3 ka ago and the Present using a clayey model, 4 km lake, 2.3 °C lake bottom temperature.

These correspond to various times including when the lake formed 13.5 ka ago, 10 ka ago, and at 9 ka ago, 7 ka ago, 3 ka ago and the present. In contrast to Taylor *et al.* [1] these *T–z* profiles correspond to the transient initial profile. The initial steady-state profile is shown for reference. Consideration of a transient temperature profile has a general but modest effect that results in higher temperatures below the lake and a more rapid dissipation of both the permafrost and GHs below the lake.

2.3.5. Positions within and Outside the Lake

All of our models considered the effect on talik formation of locations relative to the center and margins of a lake. Compared to the center of the lake these relative positions, are a very significant factor that explains, in many models, the presence or absence of the any of a talik, persistent permafrost or GH occurrences. The model predictions agree with seismic tomography analysis that are interpreted to show

the distribution of both talik and permafrost [2]. This also agrees with our models for different positions within the lake, specifically, its center, its margin and the region beyond its margin (Figure 10).

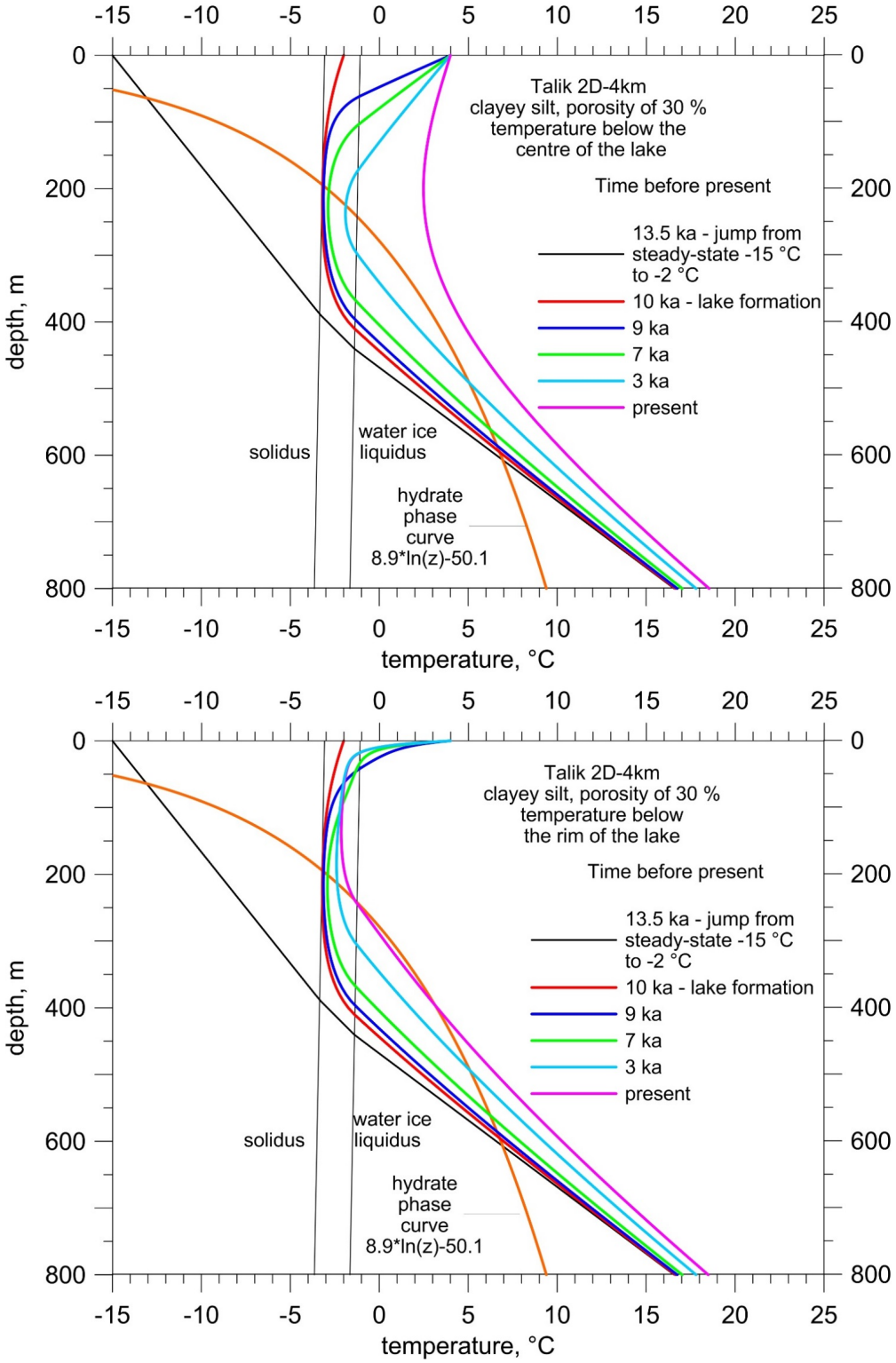

Figure 10. *Cont.*

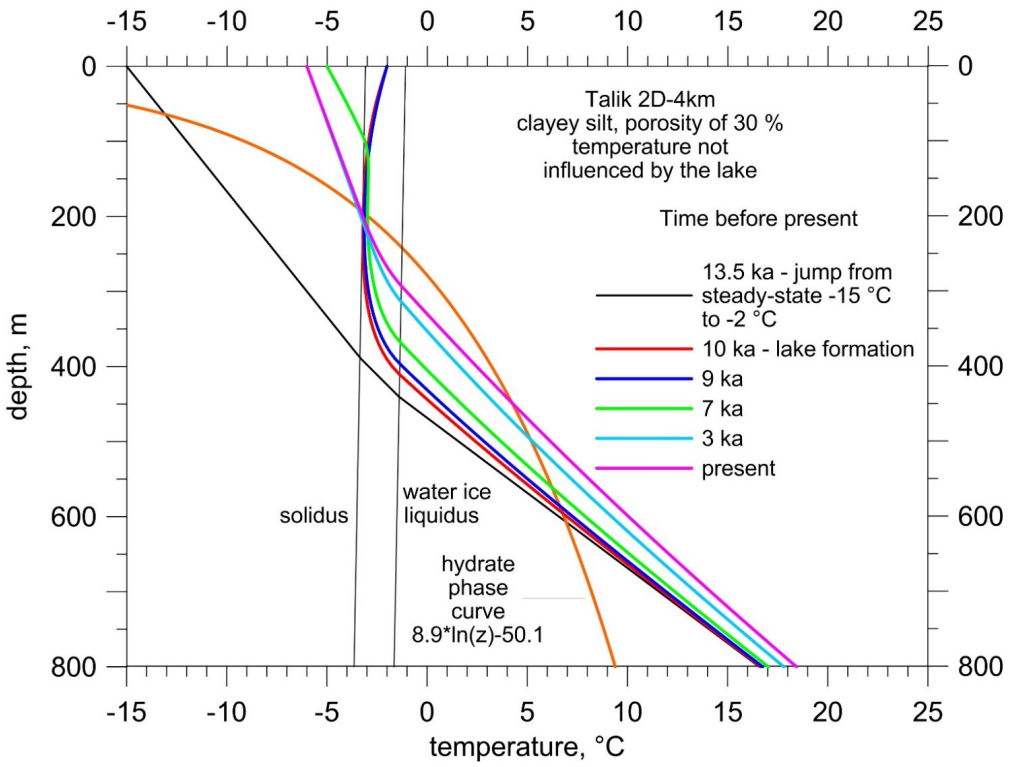

Figure 10. Illustration of the effect of position relative to the lake center for the 30% porosity clayey silt model with a 4 °C lake bottom temperature. The upper panel is the center of the lake with fully developed talik and out of GH stability zone. The middle panel is the lake's margin with permafrost temperature at or above the *solidus–liquidus* mean and marginal GH stability conditions. The lower panel is for the area beyond the margin of the lake where the lake does not influence the position of pre-existing permafrost and GH stability zone.

2.3.6. Porosity Effects

We considered also models with different porosity values, within the plausible range of the lithologies considered. This permits us to infer the maximum porosity of a clayey lithology at which the simulated present *T–z* profiles are above the *solidus–liquidus* of the ice bonded permafrost and for the GH stability zone.

This limit is found to occur at 40% porosity. Where porosities are higher, like the 48% used in [1], the permafrost does not disappear completely in the sense that part of the *T–z* profile is still in the *solidus–liquidus* zone and there is still a persistent GH stability zone below the lake even when the lake is large, the lake bottom temperature is 4 °C and the model lake formed with a transient temperature history13.5 ka ago. Below (Figure 11) are plots, that show selected results for clayey model with porosities of, 35%, 40% and 48%, for a large lake, >4 km, and a high bottom temperature of 4 °C.

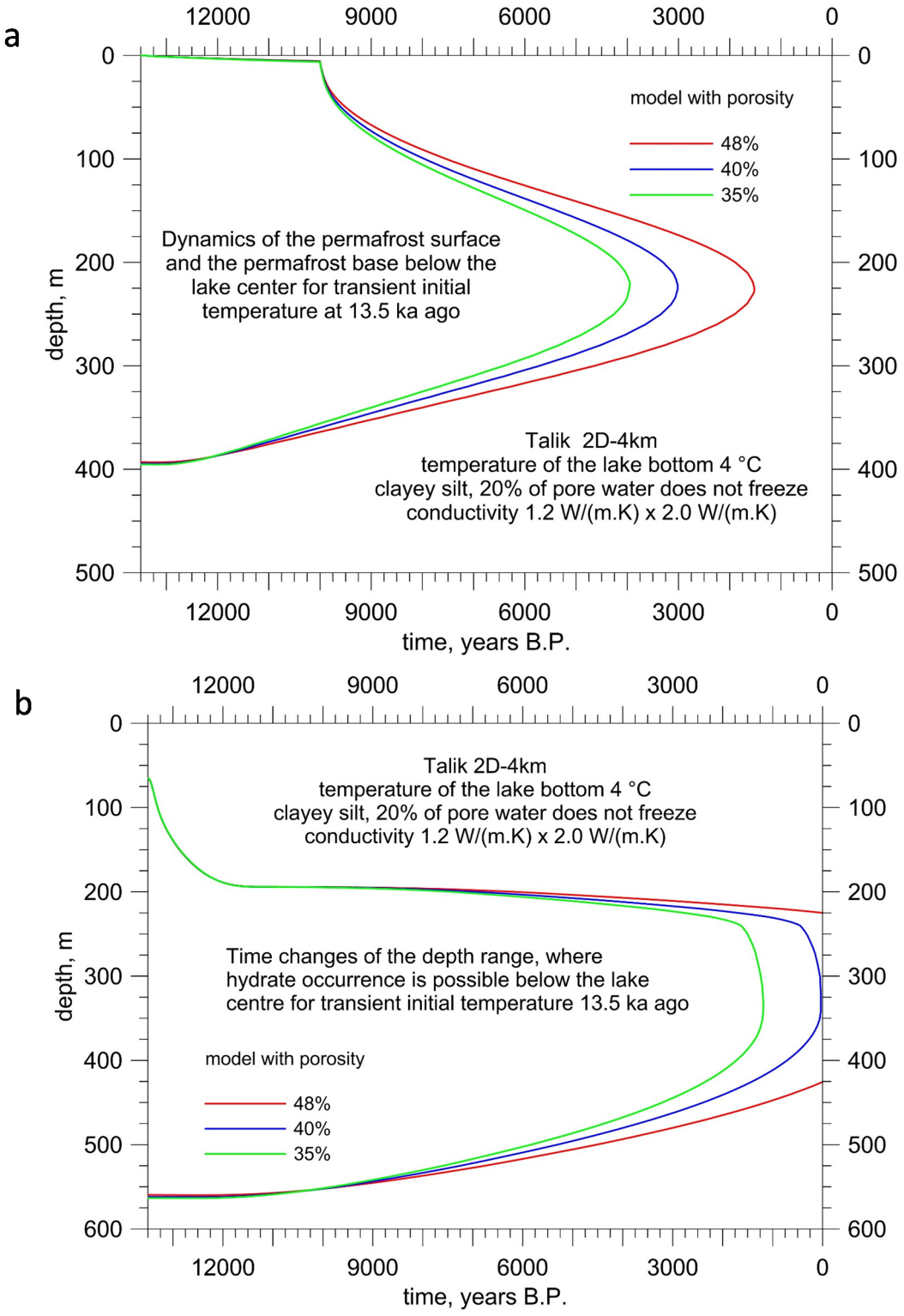

Figure 11. Influence of porosity upon permafrost (**a**) and GH stabilities (**b**) over time.

We computed the *T*–*z* profiles below the centre of the lake (corresponding to the transient initial profile) for the time when the lake formed 10 ka ago, and for 9 ka ago, 7 ka ago, 3 ka ago and the Present using the clayey silt model, a 4 km lake, a 4 °C lake bottom temperature (Figure 12). These models show that when the porosity is 35% there is no longer any GH under the lake center since at least 1 ka. At 40% porosity there is no GH and it would completely dissipated only recently. In the 48% porosity model [1], GH stability conditions continue to persist currently about 0.2–0.4 km under a 0.2 km thick talik.

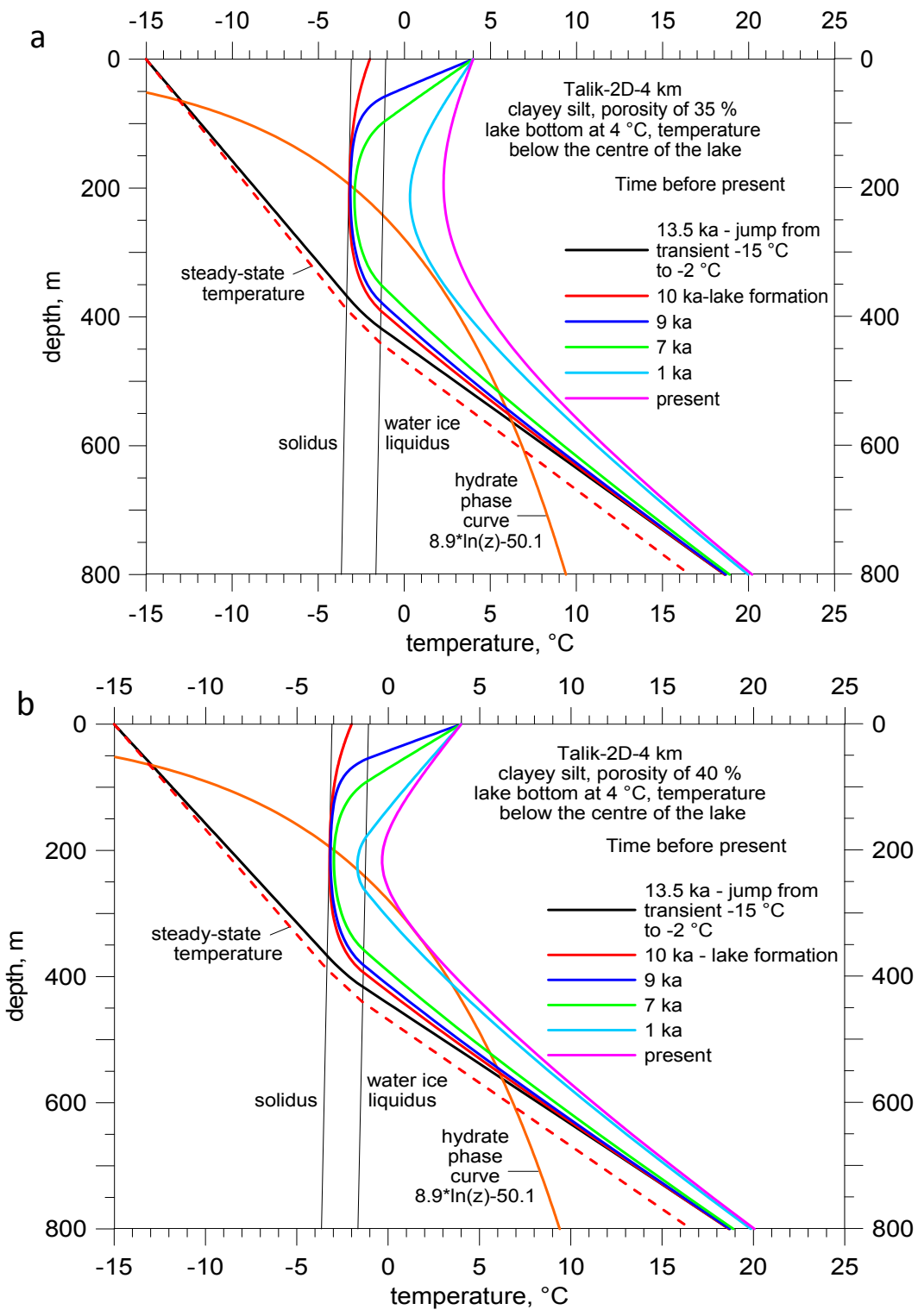

Figure 12. *Cont.*

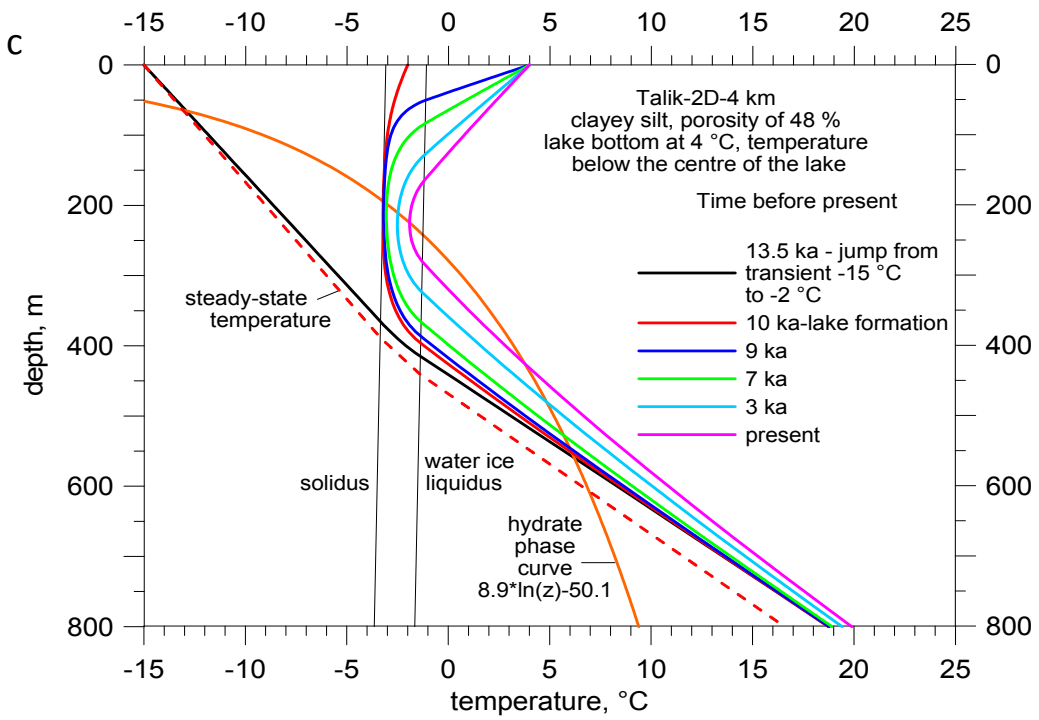

Figure 12. Computed *T*–*z* profiles below the center of the lake using the transient initial profile for a 10 ka lake with a width of 4 km and a bottom temperature of 4 °C at 9 ka ago, 7 ka ago, 3 ka ago, for clayey silt lithology with porosities of 30% (**a**), 40% (**b**), 48% (**c**).

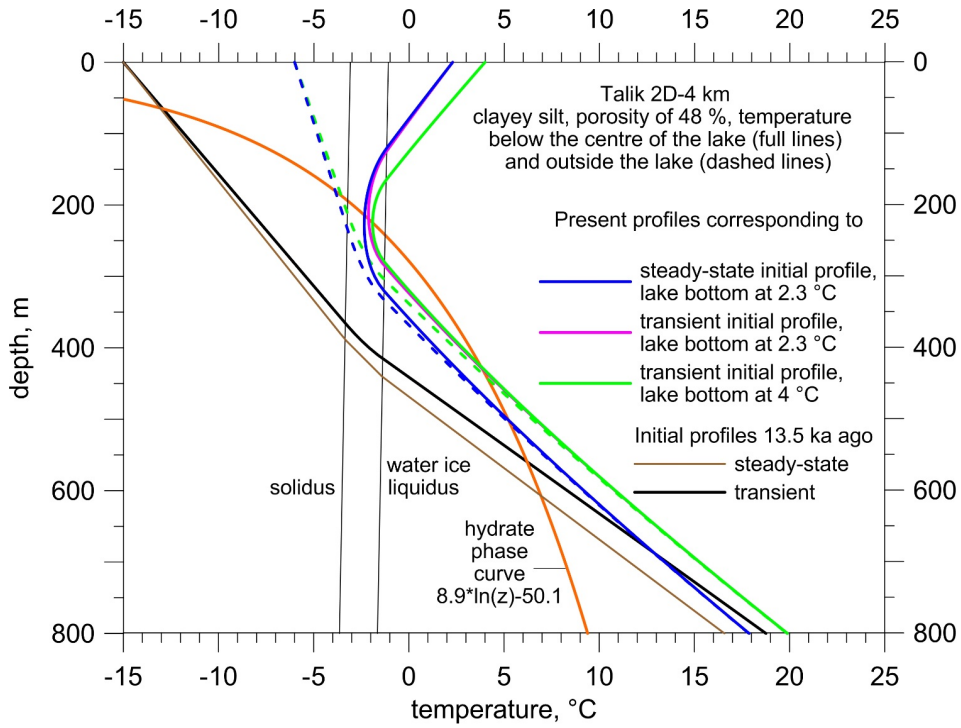

Figure 13. Current temperature–depth profiles and permafrost and GH stability for the range of temperature at the lake bottom 2.3 °C–4 °C. A model of a 2-D lake of 4 km width, 48% porosity clayey substrate for both the steady-state and transient temperature profiles.

2.3.7. The Influence of the Lake Bottom Temperature

The effect of the lake bottom temperature is shown in Figure 13. It depicts the simulated current *T–z* profiles corresponding to the lower and upper limits of the observed mean annual temperature, 2.3 °C and 4 °C, respectively [1,5].

Figure 13 shows that lake bottom temperature is important for GH stability in addition to the effects due to lithology and porosity and lake size and shape. However, the change in GH stability attributable to reasonable lake bottom temperature variations is <0.01 km. Figure 13 also shows that a change in lake bottom temperature from 2.3 °C to 4 °C increases the depth of the talik by 0.04 km, from 0.12 km to 0.16 km in this model.

3. Conclusions

The models and their analysis indicate that lithology and porosity in the sediments underlying Mackenzie Delta lakes play key roles in the control of talik formation and the persistence or disappearance of both permafrost and GH below the lakes. Models indicate that GH may persist below lakes underlain by sandy or highly porous lithology. When the underlying lithology is sandy the dissipation of both permafrost and GH below a lake of any size is practically impossible, even if a talik forms in the upper few tens of meters. Conditions of sub-lacustrine permafrost and GH occurrences resemble generally those settings where relict permafrost and GH persist under areas inundated by Holocene Beaufort Sea transgression, where GH preservation depends strongly on either underlying lithological characteristics or low sea bottom temperatures. The models indicate that permafrost degradation appears where porosities are <40% and water bottom temperatures reach 2 °C–4 °C, in both marine and lacustrine settings. The result is quite different for lakes underlain by clayey sediments, especially where they have low porosity. When the clayey lithology are little compacted (48% porosity) neither permafrost nor GHs dissipate completely below the lake. This result is similar to a case considered by other models previously [1]. However, when the clayey lithology is more compacted such that the porosity is <40%, both permafrost and GHs dissipate completely for a range of lake bottom temperatures of 2 °C–4 °C. The model results agree with seismic interpretations and drilling observations [2] that show or infer taliks present or forming under the centre of some lakes. In the Parsons Lake area permafrost is still present in Tertiary formations 0.35 km below the lake rim and its environs. Similar observations are made at other lakes like Big Lake [1] where permafrost extends some 0.3 km below the rim of the lake.

GH may occur when either sandy lithology or high porosity occurs below lakes. Such situations are similar to those where the persistent offshore relict permafrost and GHs underlie much colder water columns, therefore resolving the paradoxical relationship between the shallow Beaufort Sea, where permafrost and gas hydrates persist commonly, compared to the Mackenzie Delta where many lakes are underlain by taliks. Below those lakes with clayey silt substrates and higher lake bottom temperatures that are typical of the Mackenzie Delta, the model results match the observed dissipation of permafrost and GH stability conditions when substrate porosities are <40% and the lake bottom temperatures are 2 °C–4 °C. However, when lakes are underlain by less compacted clayey silts with >40% porosities a thinner GH stability zone can persist even where a deep talik forms. Situations where GHs persist under

a talik are inferred to be very unstable in the future when climatic warm may result in GH destabilization. GH below taliks are potentially similar to ones in shallow offshore [22–24]. It is anticipated that future climate warming will increase of sea bottom temperature provoking a future response of marine GH's, both generally or regionally, at a variety of scales [22,23].

The uncertainties related to the temperature history assumption and implication on model results depend on the validity of the assumed past surface temperature history (Figure 6). We acknowledge that the lack of temperature data means that a robust assumption on a past temperature history is rather challenging and uncertainty exists in assumed magnitude of the temperature change from glacial to interglacial (here assumed as from −15°C [1] to −2 °C at time 13.5 ka, followed outside a lake by cooling to −5 °C and −6 °C at times 8 ka and 4.5 ka, respectively. At the time of a lake origin, 10 ka, the ground temperature at the site of a lake warms up from −2 °C to +2.3 °C (or to +3 °C or +4 °). These are well researched, however, uncertain values. Warmer temperatures at Holocene could increase thickness of taliks and reduce permafrost and gas hydrates even in cases when either sandy lithology or high porosity occurs below lakes. Uncertainties in the temperature of the lake bottom [5] are important as we have shown in the above simulations (Figure 13). The formation and existence of a lake was simulated by a jump of the surface temperature from −2 °C to +2.3 °C model [1] at the site of the lake 10 ka ago. We also considered a warmer lake by changing to +3 °C or to +4 °C (See Figure 6). These simulations (Figure 13) show that lake bottom temperature is important for GH stability in addition to the effects due to lithology and porosity and lake size and shape. Therefore, farther limiting of uncertainties in the surface forcing model will be welcomed as new more precise paleo history data available in the future.

Acknowledgments

The authors would like to acknowledge the helpful reviews by two anonymous reviewers.

Author Contributions

These authors contributed equally to this work, e.g., concept, main text and figures.

Conflicts of Interest

The authors declare no conflict of interest.

Appendix

Symmetric vs. Axis-Symmetric Models and the Influence of Lake Size

We compared the model effects of lake geometry for a round 2D model against an axis-symmetric elongated lake model. We show this in Appendix Figure A1. Far away from the lake, the results provided by the 2-D (or axis-symmetric) code agree with 1-D model.

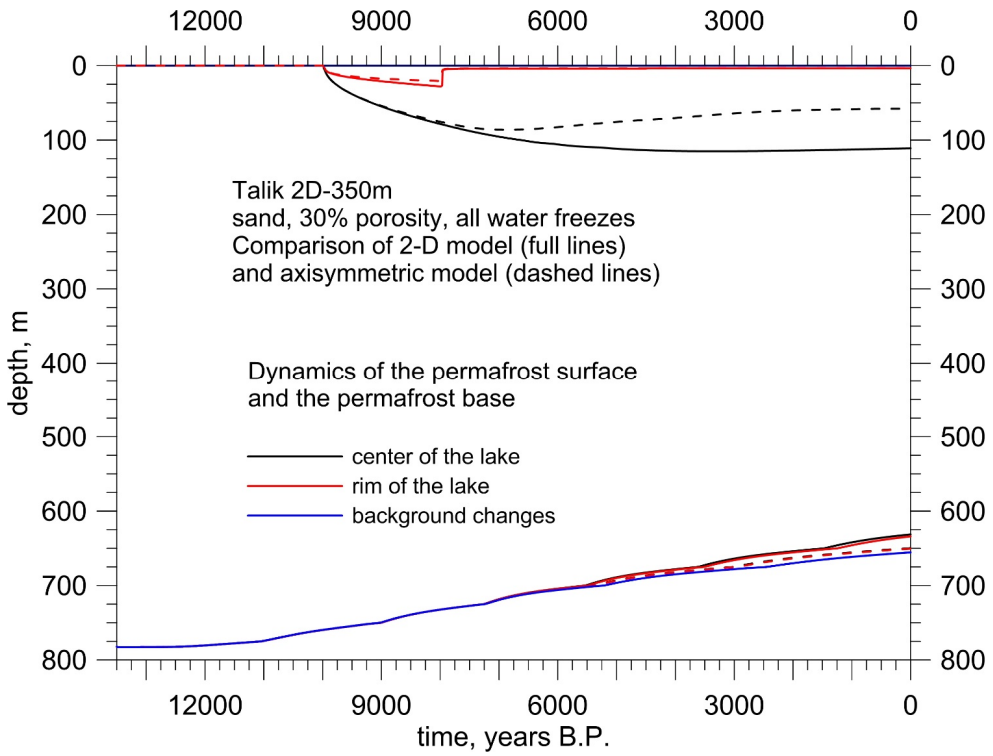

Figure A1. Comparison of 2-D infinite lake model results (full lines) with the axis-symmetric model results (broken lines).

The lake size influence is shown below (Figure A2).

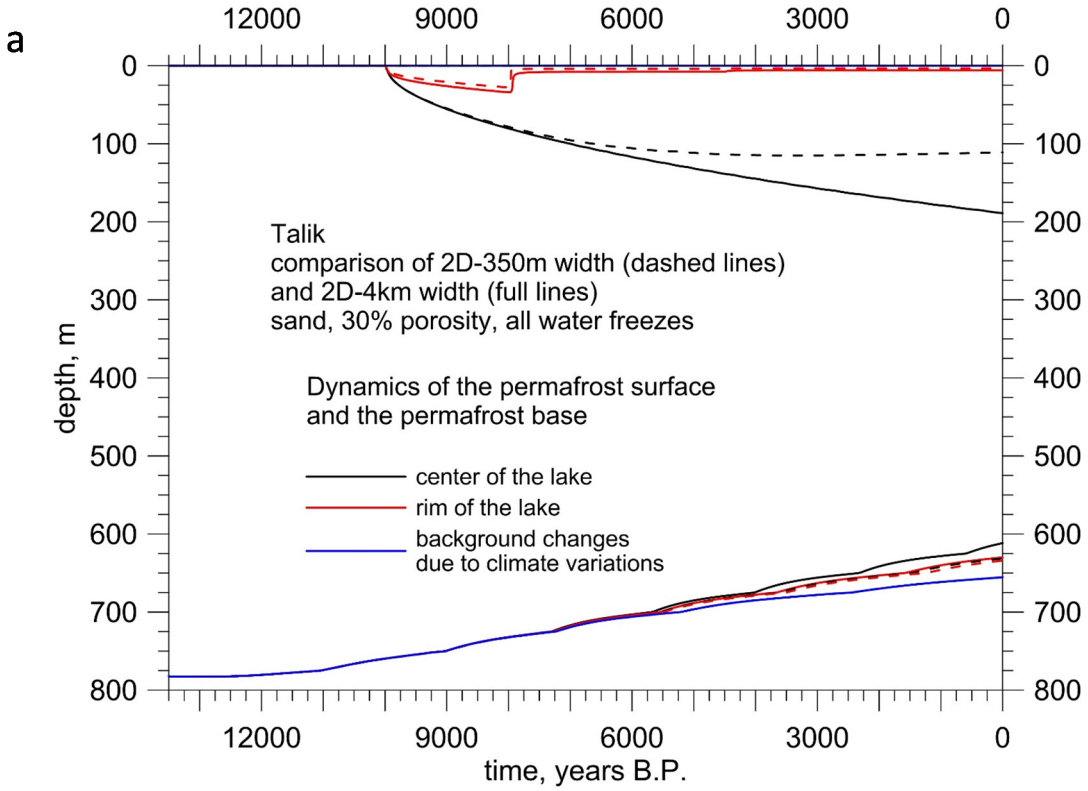

Figure A2. *Cont.*

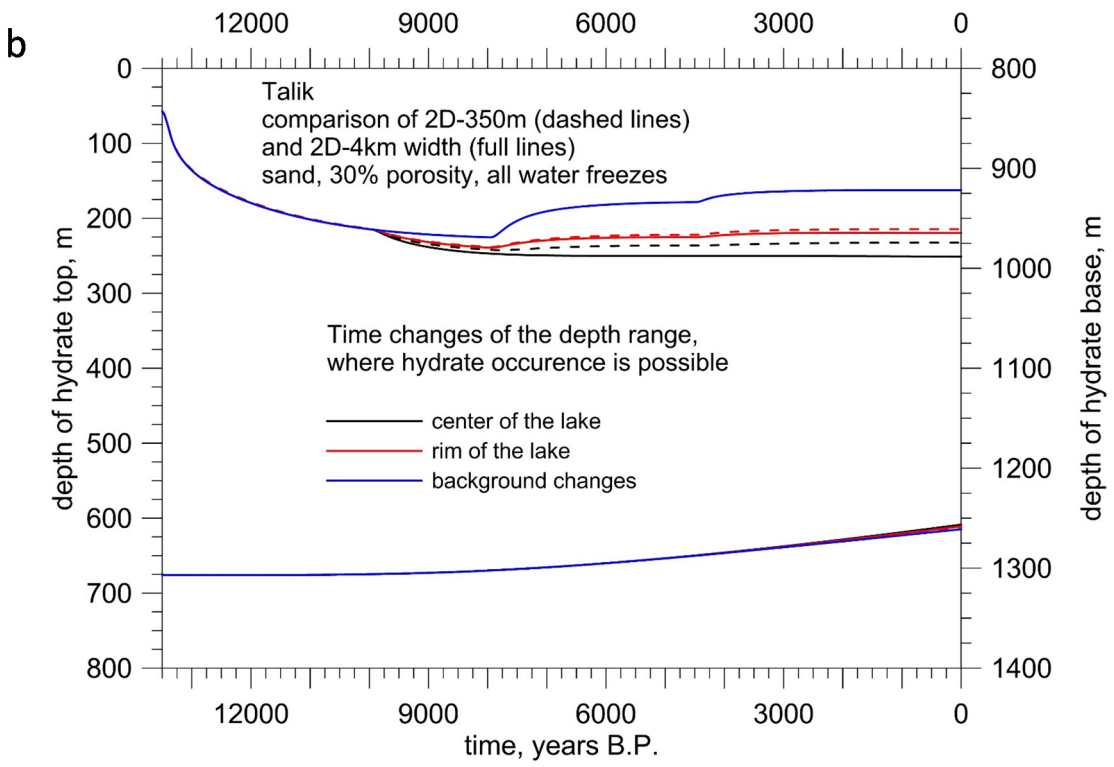

Figure A2. Temporal changes of the upper and lower boundaries of the permafrost (**a**) and methane GH layers (**b**) at: The lake's centre, rim and beyond both a small 350 m (dashed lines) and a large 4 km (solid lines) lake width.

Below (Appendix Figure A3) we illustrate the spatial changes in permafrost and GH layers for a 4 km lake calculated at 13.5 ka ago, 10 ka ago, 9 ka ago, 8 ka ago, 6 ka ago, 4 ka ago, 2 ka and the present.

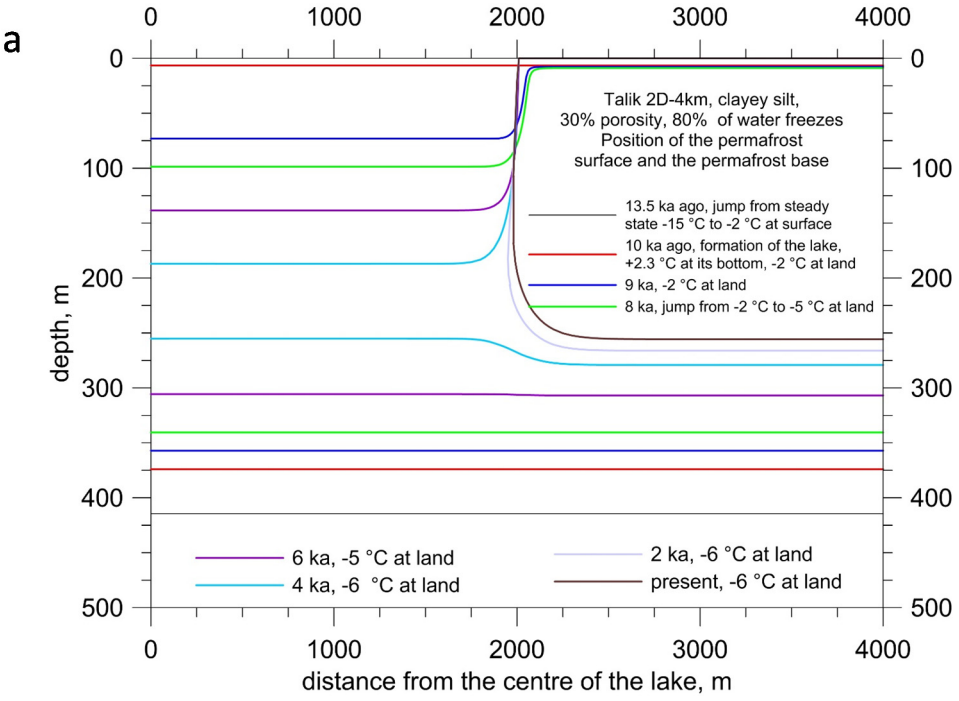

Figure A3. *Cont.*

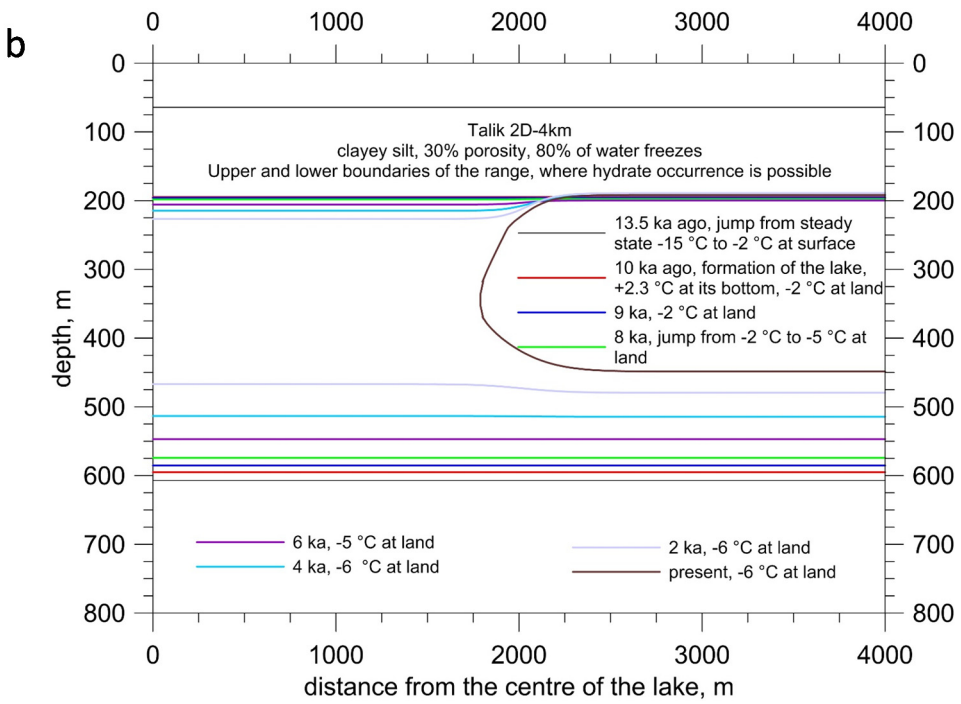

Figure A3. 4 km lake spatial and temporal changes for permafrost (**a**) and GH (**b**) for 13.5 ka ago, 10 ka ago, 9 ka ago, 8 ka ago, 6 ka ago, 4 ka ago, 2 ka and the Present.

In the next set of models we considered an even larger lake, 10 km wide, similar in size to Parsons Lake, underlain by a clayey-silt substrate with a low porosity, 30%, and a lake bottom temperature of 2.3 °C (Appendix Figure A4). We have calculated the permafrost and GH stability history and we compare the results of this larger, "Parsons Lake" model with the model of a 4 km wide lake (Figure 9).

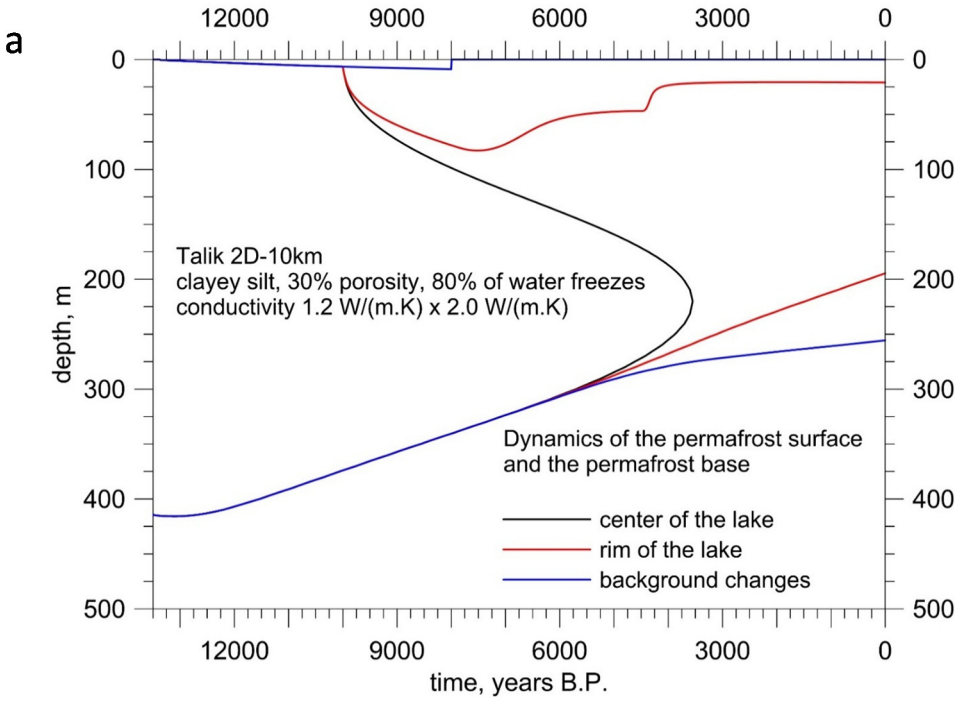

Figure A4. *Cont.*

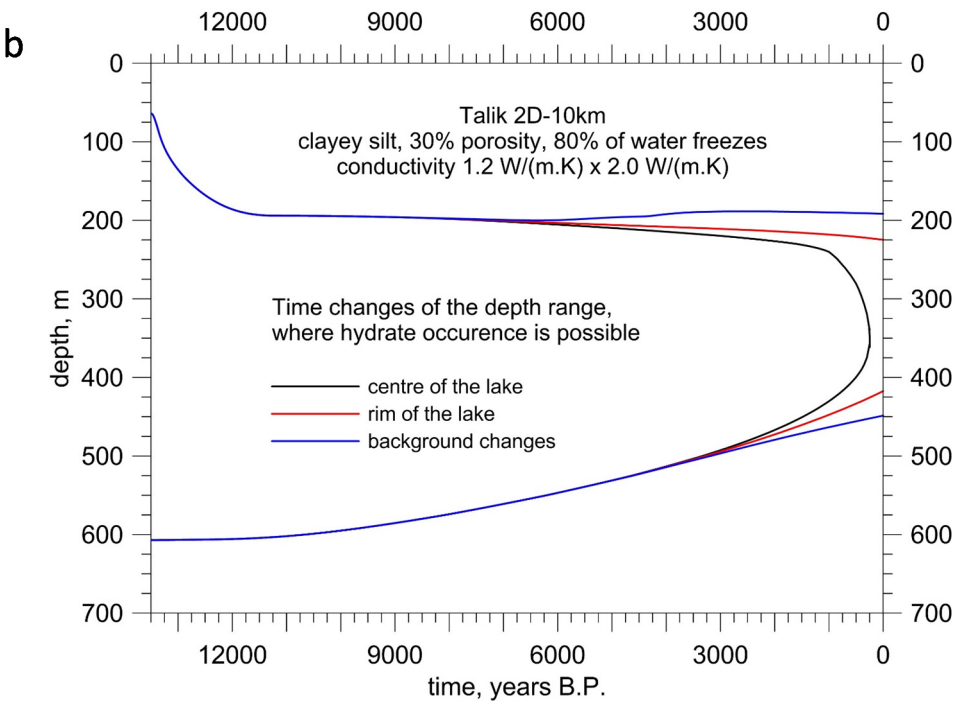

Figure A4. Variation of the permafrost (**a**) and GH (**b**) stability boundaries for a large lake, with a width of 10 km, like Parsons Lake.

References

1. Taylor, A.E.; Dallimore, S.R.; Wright, J.F. Thermal impact of Holocene lakes on a permafrost landscape, Mackenzie Delta, Canada. In Proceedings of the Ninth International Conference on Permafrost, Fairbanks, AK, USA, 28 June–3 July 2008; Kane, D.L., Hinkel, K.M., Eds.; University of Alaska Fairbanks, Institute of Northern Engineering: Fairbanks, AK, USA, 2008.
2. Bellefleur, G.; Riedel, M.; Ramachandran, K.; Brent, T.; Dallimore, S. Recent advances in mapping deep permafrost and gas hydrate occurrences using industry seismic data, Richards Island area, Northwest Territories, Canada. In Proceedings of the Frontiers + Innovation—2009 CSPG CSEG CWLS Convention, Calgary, AB, Canada, 4–8 May 2009; pp. 603–607.
3. Taylor, A.E.; Dallimore, S.R.; Judge, A.S. Late Quaternary history of the Mackenzie-Beaufort region, Arctic Canada, from modelling of permafrost temperature. 2. The Mackenzie Delta-Tuktoyaktuk coastlands. *Can. J. Earth Sci.* **1996**, *33*, 62–71.
4. Burges, M.; Judge, A.S.; Taylor, A.; Allen, D.V. Ground temperature studies of permafrost growth at a drained lake site, Mackenzie Delta (MD). In Proceedings of the 4th Canadian Permafrost Conferences, Calgary, AB, Canada, 2–6 March 1982; pp. 3–11.
5. Burns, C.R. Tundra lakes and permafrost, Richards Island, western Arctic coast, Canada. *Can. J. Earth Sci.* **2002**, *39*, 1281–1298.
6. Majorowicz, J.A.; Hannigan, P.K. Stability zone of natural gas hydrates in a permafrost-bearing region of the Beaufort-Mackenzie basin: Study of a feasible energy source. *Nat. Resour. Res.* **2000**, *9*, 3–26.
7. Osadetz, K.G.; Chen, Z. A re-examination of Beaufort Sea-Mackenzie Delta basin bas hydrate resource potential using a petroleum play approach. *Bull. Can. Pet. Geol.* **2010**, *58*, 56–71.

8. Issler, D.R.; Hu, K.; Lane, L.S.; Dietrich, J.R. *GIS Compilations of Depth to Overpressure, Permafrost Distribution, Geothermal Gradient, and Regional Geology, Beaufort-Mackenzie Basin, Northern Canada*; Geological Survey of Canada: Calgary, AB, Canada, 2009.
9. Majorowicz, J.A.; Osadetz, K.G.; Safanda, J. Modeling temperature profiles considering the latent heat of physical–chemical reactions in permafrost and gas hydrates: The MD terrestrial case. In Proceedings of the Ninth International Conference on Permafrost, Fairbanks, AK, USA, 28 June–3 July 2008; Kane, D.L., Hinkel, K.M., Eds.; Volume 2, pp. 1113–1118.
10. Majorowicz, J.A.; Osadetz, K.G.; Safanda, J. Onset and stability of gas hydrates under permafrost in an environment of surface climatic change—Past and future. In Proceedings of the 6th International Conference on Gas Hydrates (ICGH 2008), Vancouver, BC, Canada, 6–10 July 2008.
11. Šafanda, J.; Majorowicz, J.; Szewczyk, J. Geothermal evidence of very low glacial temperatures on the rim of Fennoscandian ice sheet. *Geophys. Res. Lett.* **2004**, *31*, doi:10.1029/2004GL019547.
12. Kukkonen, I.; Šafanda, J. Numerical modeling of permafrost in bedrock in northern Fennoscandia during the Holocene. *Glob. Planet. Chang.* **2001**, *29*, 259–227.
13. Carslaw, H.S.; Jaeger, J.C. *Conduction of Heat in Solids*; Clarendon Press: Oxford, UK, 1959; p. 510.
14. Lunardini, V.J. *Heat Transfer with Freezing and Thawing*; Elsevier: Amsterdam, The Netherlands, 1991; p. 437.
15. Šafanda, J. Calculation of temperature distribution in two dimensional geothermal profiles. *Stud. Geophys. Geod.* **1985**, *29*, 191–207.
16. Cermak, V.; Šafanda, J.; Kresl, M.; Kucerova, L. Heat flow studies in Central Europe with special emphasis on data from former Czechoslovakia. *Glob. Tecton. Metallog.* **1996**, *5*, 109–123.
17. Majorowicz, J.A.; Jessop, A.M.; Judge, A. S. Geothermal regime. In *Geological Atlas of the Beaufort-Mackenzie Area*; Dixon, J., Ed.; Natural Resources Canada: Calgary, AB, Canada, 1996; pp. 33–37.
18. Judge, A.S.; Smith, S.L.; Majorowicz, J.A. The current distribution and thermal stability of natural gas hydrates in the Canadian Polar Regions. In Proceedings of the Fourth International Offshore and Polar Engineering Conference, Osaka, Japan, 10–15 April 1994; pp. 307–313.
19. Majorowicz, J.A.; Grasby, S. Heat flow, depth–temperature variations and stored thermal energy for enhanced geothermal systems in Canada. *J. Geophys. Eng.* **2010**, *7*, 232–241.
20. Majorowicz, J.A.; Smith, S.L. Review of ground temperatures in Mallik field area: A constraint to the methane hydrate stability. In *Scientific Results from JAPEX/JNOC/GSC Mallik 2L-38 Gas Hydrate Research Well, Mackenzie Delta, Northwest Territories, Canada*; Dallimore, S.R., Uchida, T., Collett, T.S., Eds.; Geological Survey of Canada: Calgary, AB, Canada, 1999; Volume 544, pp. 45–56.
21. Lentz, J.; Fritz, M.; Schirrmeister, L.; Lantuit, H.; Wooller, M.; Pollard, W.; Wetterich, S. Periglacial landscape dynamics in the western Canadian Arctic: Results from a thermokarst lake record on a push moraine (Herschel Island, Yukon Territory). *Palegeogr. Paleoclim. Paleoecol.* **2013**, *381–382*, 15–25.
22. Ruppel, C.D. Methane Hydrates and Contemporary Climate Change. Available online: http://www.nature.com/scitable/knowledge/library/methane-hydrates-and-contemporary-climatechange-24314790 (accessed on 18 December 2014).

23. Giustiniani, M.; Tinivella, U.; Jakobosson, M.; Rebesco, M. Arctic ocean gas hydrate stability in a changing climate. *J. Geol. Res.* **2013**, doi:10.1155/2013/783969.
24. Majorowicz, J.; Osadetz, K.; Safanda, J. Methane gas hydrate stability models on continental shelves in response to Glacio-Eustatic sea level variations: Examples from Canadian oceanic margins. *Energies* **2013**, *6*, 5775–5806.